

## ***In situ* molecular imaging of hydrated biofilm in a microfluidic reactor by ToF-SIMS**

Xin Hua,<sup>ab</sup> Xiao-Ying Yu,<sup>\*a</sup> Zhaoying Wang,<sup>c</sup> Li Yang,<sup>c</sup> Bingwen Liu,<sup>a</sup> Zihua Zhu,<sup>c</sup> Abigail E. Tucker,<sup>d</sup> William B. Chrisler,<sup>d</sup> Eric A. Hill,<sup>d</sup> Theva Thevuthasan,<sup>c</sup> Yuehe Lin,<sup>e,f</sup> Songqin Liu,<sup>b</sup> and Matthew J. Marshall<sup>\*d</sup>

<sup>a</sup>*Atmospheric Sciences and Global Climate Change Division, Pacific Northwest National Laboratory, Richland, WA 99352. Email: xiaoying.yu@pnnl.gov; Phone: 1-509-372-4524; Fax: 1-509-372-6168*

<sup>b</sup>*School of Chemistry and Chemical Engineering, Southeast University, Nanjing, Jiangsu Province, P. R. China, 211189.*

<sup>c</sup>*W. R. Wiley Environmental Molecular Science Laboratory, Pacific Northwest National Laboratory, Richland, WA 99352.*

<sup>d</sup>*Biological Sciences Division, Pacific Northwest National Laboratory, Richland, WA 99352. Email: matthew.marshall@pnnl.gov; Phone: 1-509-371-6964; Fax: 1-509-371-6955*

<sup>e</sup>*Physical Sciences Division, Pacific Northwest National Laboratory, Richland, WA 99352.*

<sup>f</sup>*School of Mechanical and Materials Engineering, Washington State University, Pullman, WA 99164, USA*

\* Correspondence to: Xiao-Ying Yu (xiaoying.yu@pnnl.gov) and Matthew Marshall (matthew.marshall@pnnl.gov)

### **Electronic Supplementary Experimental Details**

#### *Device fabrication and interface assembly*

The silicon nitride (SiN) membrane was oxidized in an oxygen plasma for 30 sec and immediately employed to conformal contact with the polydimethylsiloxane (PDMS) block.<sup>1</sup> Irreversible bonding was formed by heating the assembly in an oven at 75 °C for 2 hr. Two 1/16" polytetrafluoroethylene (PTFE) tubings (I.D. 0.023") were interfaced to the holes on the PDMS block via two small metal tubings (New England Small Tube Inc. Litchfield, NH, USA). These connections and the original PDMS, except the SiN surface bearing the detection window, were encapsulated in a bigger PDMS block, and then coated with a thin layer of gold to reduce potential gas permeation.<sup>2</sup> A syringe pump (Harvard Apparatus, Holliston, MA, USA) was used to infuse solutions to the microfluidic reactor as needed at a maximum flow rate of 2  $\mu$ L/min. A 100 nm thick SiN membrane on a silicon (Si) frame (window: 1.5 $\times$ 1.5 mm<sup>2</sup>; and frame: 7.5 $\times$ 7.5 mm<sup>2</sup>, 200- $\mu$ m-thick, Norcada, Inc., Edmonton, Canada) was used to enclose the microfluidic channel.

#### *Biofilm growth*

All chemicals used in the chemically defined, modified M1 minimal medium were purchased from Sigma-Adrich Chemical Co. (St. Louis, MO, United States) unless otherwise noted. The modified M1 medium solution consists of piperazine-N,N'-bis(ethanesulfonic acid) (PIPES) buffer (30 mM in the starter culture or 3 mM in the microfluidic reactor) at pH 7.2, 7.5 mM sodium hydroxide, 28 mM ammonium chloride, 1.34 mM potassium chloride, 4.35 mM monobasic sodium phosphate, 30 mM sodium chloride, 0.68 mM calcium chloride, 0.005 mM

ferric nitrilotriacetic acid, and 0.001 mM sodium selenate. Wolfe's vitamins and minerals solutions were provided as described in Kieft et al.<sup>3</sup>, and the amino acids L-glutamic acid, L-arginine, and D,L-serine were supplemented at final concentrations of 2.0 mg·L<sup>-1</sup>. In the starter culture, 30 mM sodium lactate was added as the electron donor and atmospheric O<sub>2</sub> was the terminal electron acceptor. The microfluidic reactor contained 20 mM sodium lactate and 20 mM sodium fumarate as the electron donor and acceptor, respectively.

Prior to inoculating the microfluidic reactor, the reactor was sterilized by flowing a 70% ethanol solution through the system for a minimum of 3 hr. Filtered sterilized (0.22 μm) ultrapure water was passed through the system for a minimum of five volume-changes and a sterile medium solution was passed through the system overnight. To grow the starter culture, 20 mL of modified M1 minimal medium was added to a 60 mL serum bottle and sealed with a thick butyl rubber stopper. The batch starter culture was grown for 24 hours at 30° C with shaking (150 rpm). Cells were harvested by centrifugation for 10 minutes at 5000 x g at 23° C. The supernatant was decanted and the cell pellet was resuspended in 10 mL of medium optimized for the microfluidic reactor. The microfluidic reactor was inoculated as described in the main text.

To inoculate the reactor, an overnight culture of *Shewanella oneidensis* MR-1 expressing green fluorescent protein (GFP)<sup>4</sup> was harvested by centrifugation (5000 x g, 10 min) and resuspended in an equal volume of sterile medium. The resuspended bacterial culture was flown through the microfluidic reactor at 2 μL/min for 3 hr. Two 10-mL syringes containing sterile growth medium and a drip tube flow break to prevent back-contamination were aseptically attached to the manifold at the end of inoculation period. The medium solution was run through the microfluidic reactor at room temperature for five to six days at a flow rate of 2 μL/min, which was permissive for suboxic bacterial growth. In the microfluidic channel, the biofilm was adherent to the SiN membrane (Fig. 1c) and biofilm growth was confirmed by *in situ* CLSM imaging of GFP (see Fig. S1).<sup>4</sup>

#### *Biofilm drying*

The experimental setup for drying biofilms is depicted in Figure S1b. House nitrogen gas was used to blow over biofilm samples (C) sitting on a clean Si wafer in a Petri-dish (D). The nitrogen gas was introduced to the sample via a syringe (A) installed with a filter (B). The Petri-dish was covered with parafilm to minimize potential dust contamination. The syringe filter was used to prevent potential contamination from house nitrogen gas. The parafilm was perforated with small holes that provided an exit for nitrogen gas. It also served as a shield preventing laboratory air from flowing over the sample. The biofilm sample was dried completely for 1 hr. before a spot of EPS was added. The spot was added to the same location as much as humanly possible each time.

*ToF-SIMS instrumentation*

A pulsed 25 keV Bi<sup>+</sup> (beam size: ~250 nm) ion beam with an incident angle of 45 degree off the normal was used as the primary ion beam for all measurements, with the beam current of ~1.0 pA, pulse width of 130 ns and a repeated frequency of 20 kHz. No spraying or fast spreading of aqueous solutions from the aperture was observed during operation. Vacuum pressure during measurements was  $2.5\text{-}5.5 \times 10^{-7}$  mbar in the main chamber. Before each measurement, a 500 eV O<sub>2</sub><sup>+</sup> beam (~40 nA) was scanned on the SiN window with a 400×400 μm<sup>2</sup> area for ~30 s to remove surface contamination. Also, an electron flood gun was used to compensate for surface charging during all measurements. To determine the location of the aperture, high-quality SIMS images were obtained by using a 10×10 μm<sup>2</sup> imaging mode, in which the Bi<sup>+</sup> beam was scanned with 128×128 pixels with a total integration time of 65.5 s (40 shots per pixel). The average counts per pixel are about ~ 50±10. To collect high mass resolution ( $M/\Delta M \approx 2000\text{-}4000$  at  $m/z > 30$  amu) spectra from the liquid surface, a narrow pulse width (~5 ns) Bi<sup>+</sup> beam was scanned in a 2-μm diameter round area at the aperture center. Long measurement time (>20 min) was necessary to obtain spectra with reasonable quality. More ToF-SIMS measurement details were described in our previous papers.<sup>4</sup> The  $m/z$  peak intensities were integrated using the IONTOF instrument software.<sup>5,6</sup>

During PCA analysis, a matrix of raw SIMS  $m/z$  spectra data was opened within Matlab, in which the rows corresponded to different samples (*e.g.*, dried biofilm sample, uninoculated medium solution, or hydrated biofilm) and the columns consisted of selected characteristic  $m/z$  peak intensities.

## Electronic Supplementary Figures

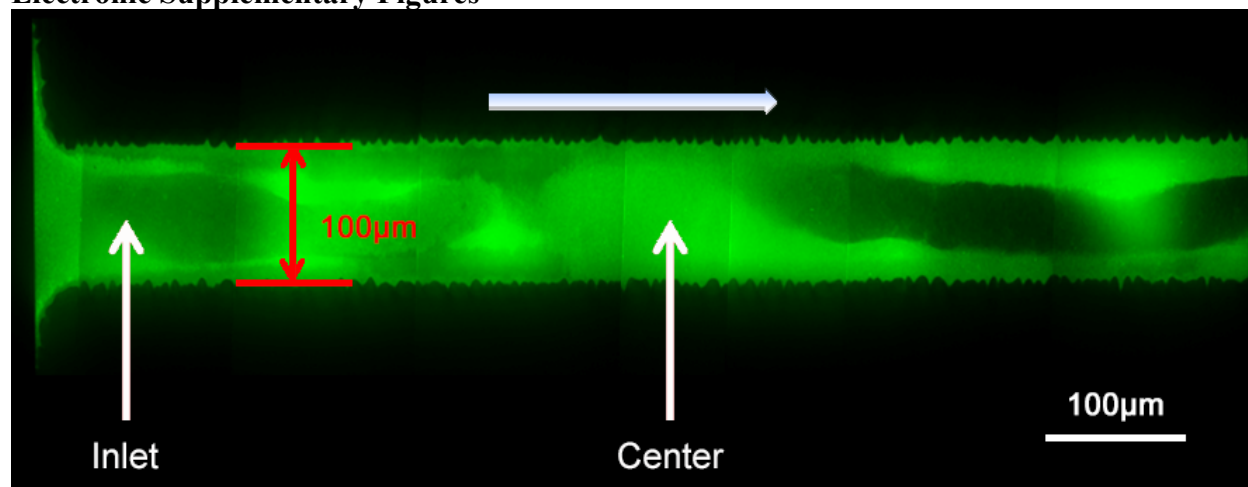


**Fig S1a.** Visualization of biofilm growth within the microfluidic channel. Confocal laser scanning microscopy (CLSM) image of *Shewanella* biofilm produced on SiN membrane in the microfluidic reactor. Cellular growth was visualized by imaging the fluorescence of the constitutively expressed cytoplasmic green fluorescent protein (GFP) (488 nm excitation; 500-550 nm emission) across the flow cell. The white arrow depicts the direction of medium flow through the microfluidic reactor. The channel width is approximately 100  $\mu\text{m}$  (y-axis). The approximate locations for ToF-SINS' depth profiling at the inlet and center of the microfluidic channel was noted using white arrows. The outlet was not shown because the CLSM images did not include the complete length of the channel. Laminar flow was used with an estimated Reynolds number of smaller than 20.

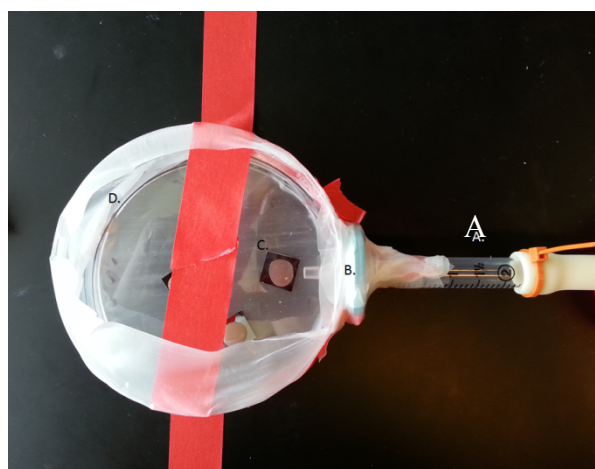


**Fig S1b.** The laboratory setup for drying the biofilm samples including A: 3 mL syringe connected to house nitrogen gas; B: 0.22  $\mu\text{m}$  filter; C: sample on Si wafer; and D: Petri-dish held open by lab tape and covered by parafilm that was perforated with small holes.

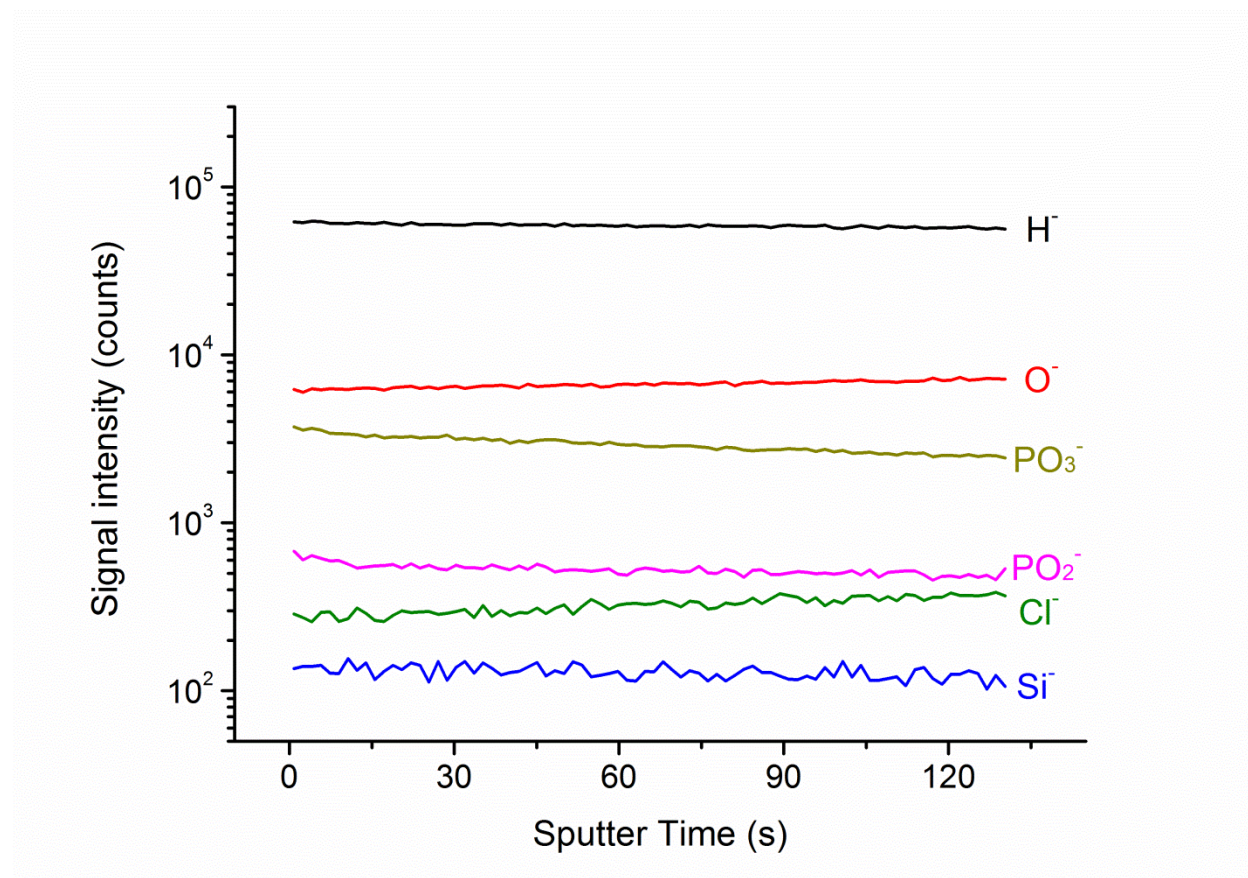


**Fig S2.** A depth profiling plot showing the signal intensity and sputter time relationship of a dried biofilm sample.

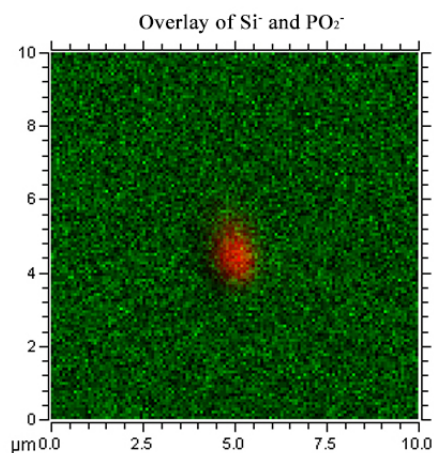


**Fig S3.** The high resolution ToF-SIMS image overlay of  $Si^-$  (green) and  $PO_2^-$  (red) in the hydrated biofilm sample. The green color illustrates  $Si^-$  signals and red color  $PO_2^-$ . The apparent size of the aperture appeared smaller than the actual size due to the superposition of the two images.

For better understanding, we drew a schematic illustration (Fig. S4) to show aperture evolution:

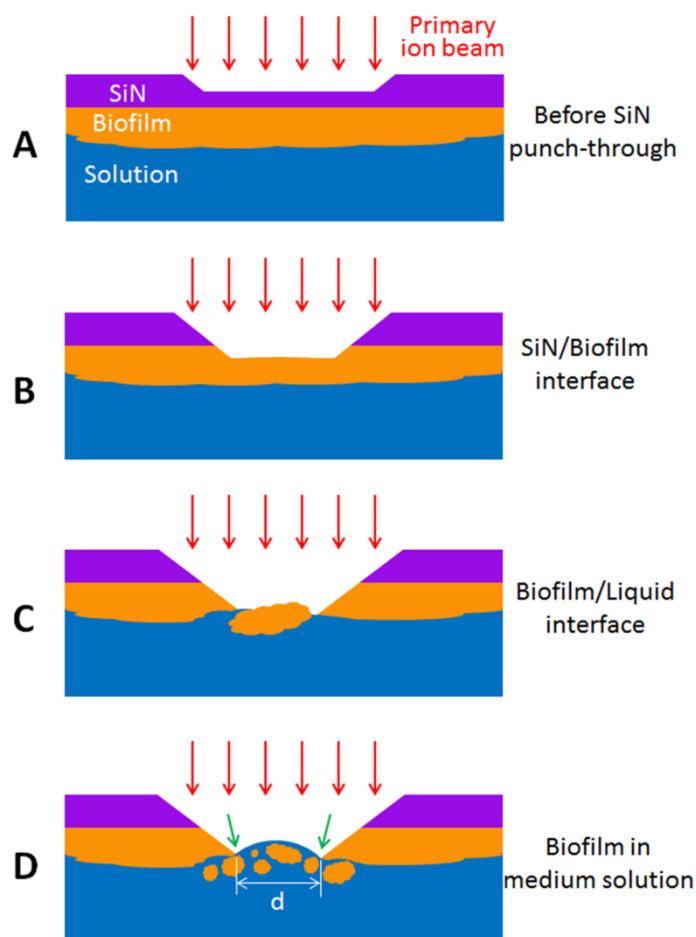


**Fig S4.** A schematic illustration of the aperture evolution during ToF-SIMS depth profiling measurements.

Figure S4 A corresponds to about the 10 s sputtering time in Fig. 3a. Some SiN material was being sputtered away. Figure S4 B corresponds to the ~60 s in Fig. 3a. The  $\text{Bi}^+$  has sputtered through the SiN layer; and the biofilm layer was being observed. Figure S4 C corresponds to ~110 s in Fig. 3a. The biofilm was getting sputtered away and some liquid was being observed due to the inhomogeneity of the biofilm thickness. Figure S4 D corresponds to ~200 s in Fig. 3a. The biofilm was drilled through. Dissolved biofilm in medium solution was observed at this time.

For the period before SiN punch-through depicted in Fig. 3a in the green shaded area, primary ion beam was continuously sputtered on the SiN membrane and gradually drilled an aperture on it, until the SiN membrane was totally drilled through, which happened on ~52 s. After that, biofilm was detected. Due to the fact that biofilm was a complex of cells, EPS, and

medium solution, the following period was considered to be a transition period in which primary ion beam continued to sputter on the biofilm layer while biofilm started to diffuse and remix with medium solution. That is, the transition covers the interface between the SiN/biofilm interface and the biofilm/liquid interface. After sputtering for 200 s, the diffusion and remixing seemed to reach a balance, corresponding to a stable state for the signal which was defined as biofilm suspended in medium solution or shortened as “biofilm in medium solution” as depicted in Fig. 3a in the orange shaded area.

The biofilm/medium solution interface may be a ring (see green arrows in Figure S4 D). This interface is highly dynamic because high  $\text{Bi}^+$  current density was used in our measurements. Meanwhile, good detection limit of SIMS ensured us to get signals of interest, such as FA C12-C16 fragments, from this interface, although the area was limited. As a result, characteristic fragments from the biofilm and medium solution interface were detected, because soluble species of interest, such as C12-C16 FAs, can diffuse from the adjacent biofilm interface to the solution.

### Electronic Supplementary Table

**Table S1.** Peak assignment of the dried biofilm sample from the negative ToF-SIMS spectra and comparison with the LIPID MAPS Structure Database (LMSD).

Common name	Species	Formula	Mass	
			LMSD	This Work
Lauric acid	$[\text{M-H}]^-$	$\text{C}_{12}\text{H}_{23}\text{O}_2^-$	199.17	199.14
Tridecylic acid	$[\text{M-H}]^-$	$\text{C}_{13}\text{H}_{25}\text{O}_2^-$	213.19	213.15
Myristic acid	$[\text{M-H}]^-$	$\text{C}_{14}\text{H}_{27}\text{O}_2^-$	227.20	227.16
Pentadecylic acid	$[\text{M-H}]^-$	$\text{C}_{15}\text{H}_{29}\text{O}_2^-$	241.22	241.18
Palmitic acid	$[\text{M-H}]^-$	$\text{C}_{16}\text{H}_{31}\text{O}_2^-$	255.23	255.18

Assignments of the dried biofilm peaks were displayed in Table S1†, in which  $m/z$  199 was attributed to  $\text{C}_{12}\text{H}_{23}\text{O}_2^-$  (lauric acid),  $m/z$  213 to  $\text{C}_{13}\text{H}_{25}\text{O}_2^-$  (tridecylic acid),  $m/z$  227 to  $\text{C}_{14}\text{H}_{27}\text{O}_2^-$  (myristic acid),  $m/z$  241 to  $\text{C}_{15}\text{H}_{29}\text{O}_2^-$  (pentadecylic acid) and  $m/z$  255 to  $\text{C}_{16}\text{H}_{31}\text{O}_2^-$  (palmitic acid). Comparison between our work and the LIPID MAPS Structure Database (LMSD, <http://www.lipidmaps.org/data/structure/>) showed slight shifts potentially due to sample uniformity and instrument responses in an experiment.<sup>7</sup> For example, the actual location of the lauric acid ( $[\text{C}_{12}\text{H}_{23}\text{O}_2]^-$ ) 199 peak is 199.14 amu which is consistent with the theoretical value (199.17 amu). For tridecylic acid ( $[\text{C}_{13}\text{H}_{25}\text{O}_2]^-$ ), the actual location of the 213 peak (213.15 amu) is in good agreement with the theoretical value (213.19 amu) (see Table S1).

### Electronic Supplementary References

1. X.-Y. Yu, B. Liu and L. Yang, *Microfluid Nanofluid*, 2013, **15**, 725-744.

2. L. Yang, Y. X.-Y., Z. H. Zhu, T. Thevuthasan and J. P. Cowin, *J. Vac. Sci. Technol. A* 2011, **29**, article no. 061101.
3. T. L. Kieft, J. K. Fredrickson, T. C. Onstott, et al., *Appl. Environ. Microbiol.*, 1999, **65**, 1214-1221.
4. J. S. McLean, *Environ. Microbiol.*, 2008, **10**, 1861-1876.
5. L. Yang, Z. Zhu, X.-Y. Yu, E. Rodek, L. Saraf, T. Thevuthasan and J. P. Cowin, *Surface Interface Analysis*, 2013, doi: 10.1002/sia5252.
6. L. Yang, Z. Zhu, X.-Y. Yu, S. Thevuthasan and J. P. Cowin, *Analytical Methods*, 2013, **5**, 2515-2522.
7. J. L. S. Lee, I. S. Gilmore, I. W. Fletcher and M. P. Seah, *Applied Surface Science*, 2008, **255**, 1560-1563.